Spatiotemporal Chaos in the Nonlinear Three-Wave Interaction

Carson C. Chow, A. Bers, and A. K. Ram

Plasma Fusion Center and Research Laboratory of Electronics, Massachusetts Institute of Technology, Cambridge, Massachusetts 02139

(Received 25 October 1991)

We examine the spatiotemporal dynamics of the nonlinear three-wave interaction describing the saturation of an unstable wave by coupling to two damped waves. We observe spatiotemporal chaos involving coherent structures that are characterized by temporal and spatial scales determined by the parameters in the problem.

PACS numbers: 05.45.+b

The nonlinear three-wave interaction (3WI) in its various guises has applications to plasma physics, nonlinear optics, and hydrodynamics [1,2]. We consider one form of the 3WI which describes the saturation of a linearly unstable parent wave by nonlinearly coupling to two damped daughter waves [2-4]. This system exhibits spatiotemporal chaos (STC). This may have implications in the saturation of stimulated Raman scattering (SRS) observed in intense laser-plasma interactions [5]. The term STC specifically refers to the chaotic dynamics of coherent structures or spatial patterns [6-9]. This is contrasted with fully developed turbulence where there is a cascade to small scales and with low-dimensional chaos where spatial degrees of freedom are not involved. The conservative form of the 3WI is integrable by inverse scattering transforms (IST) and has soliton solutions [1,10,11]. We consider the nearly integrable limit of the 3WI and use numerical simulations and perturbation theory about the IST solutions to gain some understanding of the dynamics.

The 3WI is a ubiquitous interaction that can occur whenever three linear waves are in resonance in a weakly nonlinear medium [1,2,4,12]. We studied the dynamics of the 3WI in one spatial dimension x and time t. For weakly growing and damped waves the 3WI has the form [2-4]

$$\partial_t a_i - D\,\partial_{xx} a_i - \gamma_i a_i = -a_j a_k\,, \tag{1a}$$

$$\partial_t a_j - \partial_x a_j + \gamma_j a_j = a_i a_k^*\,, \tag{1b}$$

$$\partial_t a_k + \partial_x a_k + \gamma_k a_k = a_i a_j^*\,, \tag{1c}$$

where the a's are complex wave envelopes, the γ's are growth or damping coefficients, and D is a diffusion coefficient. The diffusion term is usually not included in the 3WI. This term arises if we assume that the growth of the linear wave has a slow spatial variation. It is then the lowest-order reflection invariant term that provides a cutoff in wave number of the growth. It will become apparent later that this term is essential for nonlinear saturation and is very important in determining the long time behavior [13]. The subscript i denotes the high-frequency unstable parent wave. The other two waves are referred to as the daughters. We have transformed to the frame of the parent wave and normalized the magnitude of the daughter group velocities to unity. We will consider the case where the daughter waves have equal damping (i.e., $\gamma_j = \gamma_k$). The length and time can then be rescaled so that the damping coefficient is unity. The group velocities satisfy the condition $v_k > v_i > v_j$ (i.e., the highest-frequency parent wave has the middle group velocity, see [14]). In the absence of growth, damping, and diffusion ($\gamma_l = D = 0$) the IST solution for this group velocity ordering is described by soliton exchange between wave packets [1,10,11,15].

We numerically simulated the system on the domain $x \in [0,L)$ with periodic boundary conditions. We began with random real initial conditions and evolved until the transients died away before the system was analyzed. It can be shown that for real valued initial conditions the envelopes remain real for all time [1,4]. We were interested in the large system, long time limit. We considered the case with parameters $D=0.001$, $\gamma_i=0.1$, $\gamma_j=\gamma_k=1$, and $L=20$. These parameters were chosen because they exhibit STC and fall into a regime where perturbation theory is possible. However, the system is extremely rich and different parameters do lead to vastly different behavior. Aspects of these different regimes will be touched upon later and details are given in [4]. We measured the correlation function, $S_l(x,t) = \langle a_l(x-x',t-t')a_l(x',t')\rangle$, where the angular brackets denote time averages.

A sample of the spatiotemporal evolution profiles in the STC regime of the parent and daughter envelopes is given in Fig. 1. The length shown is one-half the system size and $t=0$ is an arbitrary time well after the transients have decayed. The profile of the parent wave is irregular but spatial and temporal scales can be observed. There are coherent structures of a definite length scale that can be seen to grow, deplete, and collide with one another. The profile of the daughter wave shows a sea of structures convecting to the left. We only show one daughter; the other will be similar but with structures convecting to the right. Figure 2 shows the spectrum of static fluctuations $S_l(q,t=0)$. For the parent wave there is a cutoff near $q \simeq 10$ and a range of modes show up as a prominent hump. The cutoff reflects the length scale seen in the

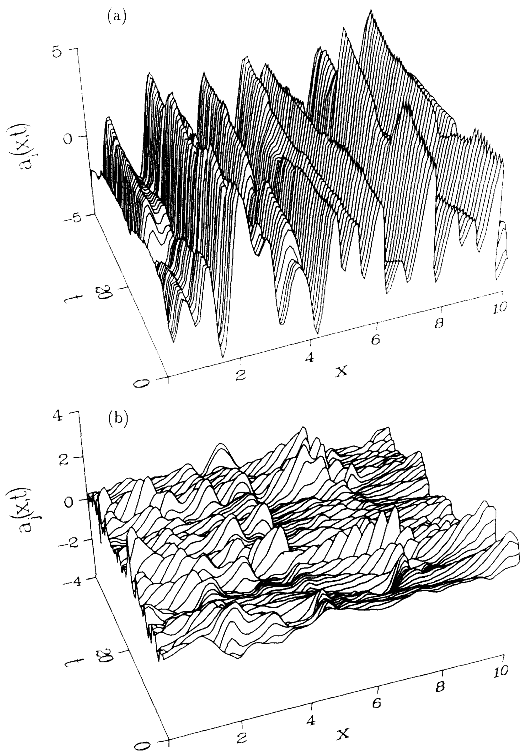

FIG. 1. Spatiotemporal profiles of (a) the parent wave $a_i(x,t)$, and (b) the daughter wave $a_j(x,t)$.

spacetime profile. For q below the hump the spectrum is flat. The daughter spectrum has a softer cutoff around $q \simeq 6$ again indicating a length scale, although not as well defined. Figure 3 shows the local power spectrum $S_l(x=0,\omega)$. The spectrum for the parent clearly shows two time scales. The spectrum bends over near $\omega \simeq 0.02$ which gives a long time scale and a shoulder at $\omega \simeq 0.3$ gives a short time scale. Longer runs with these parameters hint that there may be a very slow power-law rise of undetermined exponent for frequencies below the low ω bend similar to that observed in the Kuramoto-Sivashinsky equation [6]. The short time scale appears as the growth and depletion cycle observed in the spatiotemporal profile in Fig. 1. The daughter power spectrum has two peaks at high ω: One is where the shoulder of the parent spectrum is and the other is at twice this frequency. The spectrum begins to bend over at $\omega \simeq 0.007$. This bend is more pronounced in longer runs. It is not known whether the spectrum becomes flat or has a power-law rise like the parent for frequencies below the bend.

The main features of the behavior can be understood if we consider the growth and dissipation as perturbations about the conservative 3WI. The IST solutions for the conservative case on the infinite domain show that solitons exist but they do not necessarily belong uniquely to a particular envelope [1,10,15]. Solitons in the parent wave tend to deplete to solitons in the daughters which propagate away. The simplest soliton solution for decay shows

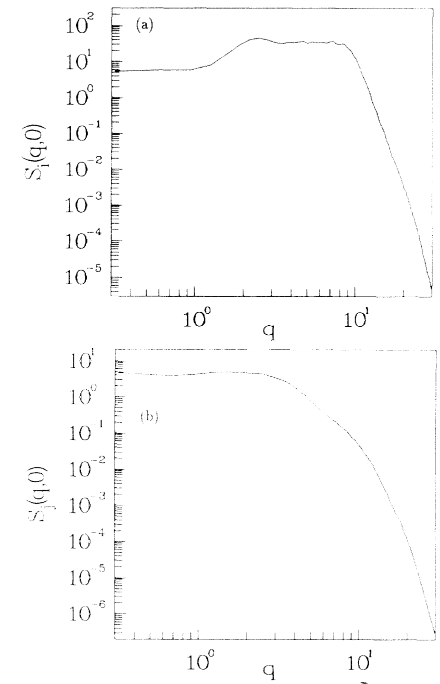

FIG. 2. Spectrum of static fluctuations $S_l(\tilde{q},t=0)$ of (a) the parent wave, and (b) the daughter wave.

that a soliton of the form $|a_i| = 2\eta\,\mathrm{sech}(2\eta x)$ will decay into solitons in each of the daughters of the form $|a_l| = \sqrt{2}\eta\,\mathrm{sech}[\eta(x+v_l t)]$, where η is the IST spectral parameter for the Zakharov-Manakov [11] scattering prob-

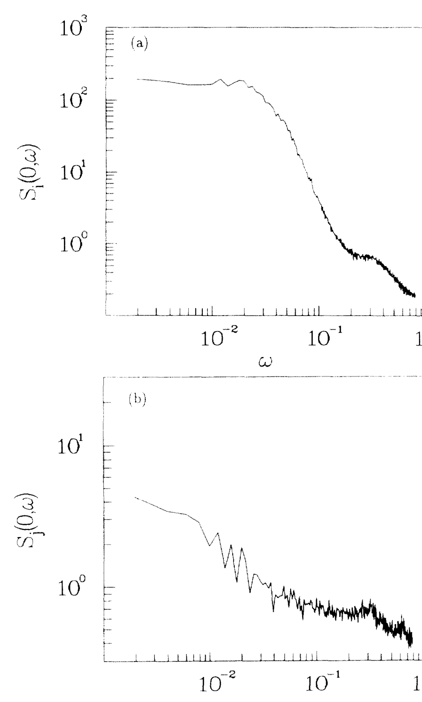

FIG. 3. Local power spectrum $S_l(x=0,\omega)$ of (a) the parent wave, and (b) the daughter wave.

lem. The spectral parameter is also the eigenvalue for a bound state in the Zakharov-Shabat [16] scattering problem with the parent pulse as the potential function. In the WKB limit η is related to the area of the parent pulse through the Bohr quantization condition [1,3,16]

$$\int_a^b |a_i^2-\eta^2|^{1/2}dx=\pi/2\,, \tag{2}$$

where $[a,b]$ are turning points for a local pulse. A collision between a daughter pulse and a parent soliton is necessary to induce the decay of the parent [1,15]. For arbitrary shaped parent pulses that exceed the area threshold, the soliton content will be transferred to the daughters leaving the radiation behind. Collisions between daughter solitons are elastic.

With the addition of weak growth and dissipation, parent pulses deplete provided they satisfy the WKB threshold condition [3,17]

$$\int_a^b |a_i^2-\gamma_j^2|^{1/2}dx>\pi/2\,. \tag{3}$$

The decay products in the daughters are quasisolitons; they damp as they propagate away and do not collide elastically. The soliton content of the parent is not completely transferred to the daughters. The parent wave with some initial local eigenvalue η will deplete and be left with some remaining area. This area is due to the conversion of soliton content into radiation by the perturbations. This left over area can be represented by an effective "eigenvalue" η'. This remaining part of the parent will then grow until it exceeds the threshold for decay. This time denoted by t_c is given by

$$t_c\simeq(1/\gamma_i)\ln(\eta/\eta')\,. \tag{4}$$

The cycling time observed in the spacetime profiles is this time plus the time required to deplete. The depletion time from IST theory is on the order $1/2\eta$ and for $\gamma_i\ll 2\eta$ this can be neglected and t_c gives the cycling time. By treating the damping and growth as a slow time scale perturbation of the IST soliton decay solution described above and ignoring the effects of diffusion on this short time scale, a multiple-time-scale perturbation analysis about the IST soliton solution was used to estimate η'. In this calculation the ordering $\gamma_i\ll\gamma_j\ll 2\eta$ was chosen. The small parameter is $\gamma_j/2\eta$ but by simply rescaling in time and space either γ_j or η can be scaled to $O(1)$. To leading order this yields [4]

$$\eta'\simeq\gamma_j\,. \tag{5}$$

The derivation assumes that the decay time for a soliton is much faster than the growth and damping time. Simulations for parent soliton initial conditions verify Eq. (5) [4]. In order to complete the calculation for the cycling time t_c it is necessary to estimate the threshold local η required for decay. By comparing the Bohr quantization condition (2) with the WKB condition for decay with damping (3) we know that $\eta>\gamma_j$. Using the IST scattering space perturbation theory developed by Kaup [1,18,19] and recently reviewed in Ref. [20], we constructed the time dependence of the IST scattering data due to the perturbations. The same ordering as the multiple scale calculation was chosen. From this we were able to estimate η to leading order to be [4]

$$\eta\simeq 2\gamma_j+4\xi_p\gamma_i\,, \tag{6}$$

where ξ_p is the parent correlation length and will be defined later. Equation (6) is sensitive to the amplitudes of the colliding daughter waves that induce the decay. The calculation assumes the decay is induced by collisions with quasisolitons with the same phase from each daughter generated two correlation lengths away. The relative phases of the colliding daughters is very important. If we consider real amplitudes, Eq. (1a) shows that two daughter quasisolitons with opposite signs (phase) actually reinforce the parent rather than make it deplete. Thus expression (6) should be considered more of a lower bound. In the simulation, radiation and diffusive effects will be relevant and may also further delay the decay of the parent. From η we are able to estimate the daughter correlation length. This is given by the quasisoliton width $\xi_d\simeq 2/\eta$.

The long time behavior is governed by the diffusion. The trivial fixed point of Eq. (1) is given by

$$\partial_{xx}a_i+q_0^2a_i=0,\quad a_j=a_k=0\,, \tag{7}$$

where $q_0=(\gamma_i/D)^{1/2}$. Modes with $q>q_0$ will damp and those with $q<q_0$ will grow. Thus the fixed point is always unstable to long wavelength fluctuations. However, when a local area between two turning points of the parent wave contains a bound state with eigenvalue η it will deplete. In the depletion process broad parent pulses will be decimated. The growth in the $q<q_0$ modes are thus saturated nonlinearly. This results in long wavelength distortions beyond lengths $2\pi/q_0$. The principle mode q_0 was observed as the cutoff in the spectrum of static fluctuations [Fig. 2(a)]. The mode q_0 defines the correlation length for the parent, $\xi_p\simeq 2\pi/q_0$. If $D=0$ there will not be any nonlinear saturation of the instability because q_0 would become infinite and so would the amplitude required to fulfill the area threshold (3).

The long time scale for the parent τ_p is given by the diffusion time across a length ξ_p giving $\tau_p\simeq(2\pi)^2/\gamma_i$. This is the time scale in which the local parent structures will shift position, collide with other structures, or diffuse away. The long correlation time observed in the daughters is associated with the interaction of the daughter quasisolitons with the parent structures. Whenever quasisolitons collide with the parent structures they may induce a decay and create a new quasisoliton where the collision occurred. This would lead to a long correlation time for the daughters. As the parent structures drift so would the creation location of new quasisolitons. However, because the quasisolitons have a different width than the parent structures, the long time scale for the daughters would be given by the diffusion time across a quasisoliton width yielding $\tau_d \simeq 4/\eta^2 D$. The newly created quasisoliton damps while it continues to propagate along the characteristic. However, when it collides with another parent structure it could induce a decay and repeat the process. The parent structures act as amplifiers regenerating damped quasisolitons that collide with them.

Using the above analysis for the parameters of the simulation we obtain the following estimates: $\tau_p \simeq 400$, $q_0 = 10$, $\xi_p \simeq 0.6$, $\eta' \simeq 1$, $\eta \simeq 2.2$, $t_c \simeq 8$, $\xi_d \simeq 0.9$, and $\tau_d \simeq 800$. These estimates corroborate fairly well with the simulation. The estimate for t_c is a bit low compared to the shoulder in the parent power spectra at $\omega \sim 0.3$ corresponding to $t \simeq 20$. However, the spacetime profiles in Fig. 1 do show some of the parent structures cycling near the predicted time scale, so the calculation does predict a lower bound.

A word should be said about the system size. It is clear with the very long correlation times for the daughters that they cycle the box many times before correlations decay away. Thus for long times, the temporal correlation function along the characteristic or at a single spatial location would be the same. This was borne out in the simulation. It is unknown what the precise boundary effects are since it would be impossible to numerically test a system large compared to this long time scale. However, with other runs of varying length, it was found that the above time scales seem to be unaffected by the system size as long as it is much larger than ξ_p. The power-law rise for the parent power spectrum below $2\pi/\tau_p$ seems to decrease in exponent as the system size increases.

We chose parameters where perturbation theory about the IST solutions could be applied to try to understand the dynamics. However, the behavior does dramatically change for different parameter regimes [4]. For strong growth rates, the long time scales observed tend to disappear and only the growth and depletion cycling time is evident. The parent grows strongly and depletes violently preventing the structures from becoming established. The larger the growth rate the larger the amplitudes of the quasisolitons [4]. Another regime is when the diffusion is large so the parent structures are much broader than the damping length of the daughters. In this situation the daughters grow and damp within the confines of a parent pulse. Spatial exchange of information between these pulses is very slow. These and other regimes are reported in Ref. [4]. It is quite clear that the 3WI in spacetime is an extremely rich system. For weak growth and dissipation, it exhibits STC and perturbation theory is able to estimate the length and time scales.

The spectral broadening and amplitude saturation of the unstable wave occurs for almost all parameters and is independent of the order of the group velocities. As an application we have considered the saturation of SRS due to decay of the electron plasma wave (EPW) [4]. The unstable EPW in SRS can decay rapidly to another EPW and ion-acoustic wave. The ensuing STC [4] broadens the spectrum and saturates this EPW which, for a fixed input laser power, leads to [2] the saturation of the scattered wave in SRS. Further details will be given in an upcoming publication.

One of us (C.C.) wishes to thank T. Hwa and D. Kaup for fruitful and interesting discussions. This work was supported in part by NSF Grant No. ECS-88-2475, LLNL subcontract No. B160456, and DOE Grant No. DE-FG02-91ER-54109.

[1] D. J. Kaup, A. Reiman, and A. Bers, Rev. Mod. Phys. **51**, 915 (1979), and references therein.

[2] A. Bers, in *Plasma Physics–Les Houches 1972*, edited by C. De Witt and J. Peyraud (Gordon and Breach, New York, 1975).

[3] Carson C. Chow, A. Bers, and A. K. Ram, "Research Trends in Chaotic Dynamics and Transport in Fluids and Plasmas," AIP Conference Proceedings (American Institute of Physics, New York, to be published).

[4] Carson C. Chow, Ph.D. thesis, Department of Physics, Massachusetts Institute of Technology, 1991 (unpublished).

[5] S. H. Batha, D. S. Montgomery, K. S. Bradley, R. P. Drake, K. Estabrook, and B. A. Remington, Phys. Rev. Lett. **66**, 2324 (1991).

[6] P. C. Hohenberg and B. I. Shraiman, Physica (Amsterdam) **37D**, 109 (1989), and references therein.

[7] P. Coullet, C. Elphick, and D. Repaux, Phys. Rev. Lett. **58**, 431 (1987).

[8] F. T. Arrechi, G. Giacomelli, P. L. Ramazza, and S. Residori, Phys. Rev. Lett. **65**, 2531 (1990).

[9] S. Ciliberto and M. Caponeri, Phys. Rev. Lett. **64**, 2775 (1990).

[10] D. J. Kaup, Stud. Appl. Math. **55**, 9 (1976).

[11] V. E. Zakharov and S. V. Manakov, Pis'ma Zh. Eksp. Teor. Fiz. **18**, 413 (1973) [JETP Lett. **18**, 243 (1973)].

[12] D. J. Benney and A. C. Newell, J. Math. Phys. **46**, 133 (1967).

[13] An equivalent set of 3WI equations can be written in two spatial dimensions (e.g., x and y) for nonlinear interactions in the steady state [1]; the equations are of the same form as (1) where t is y and, in each equation, all other terms are divided by the y component of the group velocity of the wave. Thus the solutions we describe (x,t) apply also to (x,y) with appropriate boundary conditions.

[14] In the two-dimensional steady state, see [12] above, this condition involves only the ratios of group velocity components.

[15] A. Bers, D. J. Kaup, and A. H. Reiman, Phys. Rev. Lett. **37**, 182 (1976).

[16] V. E. Zakharov and A. B. Shabat, Zh. Eksp. Teor. Fiz. **61**, 118 (1971) [Sov. Phys. JETP **34**, 62 (1971)].

[17] A. Bers, in *Handbook of Plasma Physics*, edited by M. N. Rosenbluth and R. Z. Sagdeev (North-Holland, Amsterdam, 1983), Vol. 1, Chap. 3.2.

[18] D. J. Kaup, SIAM J. Appl. Math. **31**, 121 (1976).

[19] D. J. Kaup and A. C. Newell, Proc. R. Soc. London A **361**, 413 (1978).

[20] Y. S. Kivshar and B. A. Malomed, Rev. Mod. Phys. **61**, 763 (1989).